

**GROWTH AND CHARACTERIZATION OF PD/SIO<sub>2</sub>/ZNO  
NANORODS FOR ELECTRICALLY PUMPED RANDOM  
LASER**

**KEVIN OOI ZHENG**

**UNIVERSITI SAINS MALAYSIA**

**2023**

**GROWTH AND CHARACTERIZATION OF PD/SIO<sub>2</sub>/ZNO  
NANORODS FOR ELECTRICALLY PUMPED RANDOM  
LASER**

by

**KEVIN OOI ZHENG**

**Thesis submitted in fulfillment of the requirements  
for the degree of  
Master of Science**

**May 2023**

## **ACKNOWLEDGEMENT**

First and foremost, I would like to express my deep and sincere gratitude to my research supervisor, Dr Mohd Mahadi Halim for his guidance throughout this work. This thesis would not be completed without his support. His dynamism, vision, sincerity and motivation have deeply inspired me. He has taught me the methodology to carry out the research and to present the research works as clearly as possible. It was a great privilege and honor to work and study under his guidance. I am extremely grateful for what he has offered me especially through his research grant under the Ministry of Higher Education Malaysia which is the Fundamental Research Grant Scheme with Project Code: FRGS/1/2020/STG07/USM/02/10. Also, I am extending my thanks to my co-supervisor, Dr Marzaini Mohd Rashid for helping me with the experiment. I am extremely grateful to my senior Nurizati Rosli for teaching me how to use the equipment and how to write paper and thesis. Her patience and kindness while helping me in experiments are very much appreciated. I would like to say thanks to my friends and research colleagues, Atiqah, Ainita, Suvind and Puteri for their constant encouragement. I would also express my special thanks to all the lab assistants for their genuine support throughout this research work. Finally, I would like to thank my dad Ooi Say Hoe, my mom Goh Ouay Lee, my brothers Ooi Shangyan and Ooi Yanjie. My journey from the beginning till the end of my master studies would not be possible without the help and support, care, and concern from my family members. They have been one step behind me all the way, always.

## TABLE OF CONTENTS

<b>ACKNOWLEDGEMENT.....</b>	<b>ii</b>
<b>TABLE OF CONTENTS.....</b>	<b>iii</b>
<b>LIST OF TABLES.....</b>	<b>vii</b>
<b>LIST OF FIGURES.....</b>	<b>viii</b>
<b>LIST OF SYMBOLS.....</b>	<b>xiv</b>
<b>LIST OF ABBREVIATIONS.....</b>	<b>xvii</b>
<b>LIST OF APPENDICES.....</b>	<b>xx</b>
<b>ABSTRAK.....</b>	<b>xxi</b>
<b>ABSTRACT.....</b>	<b>xxiii</b>
<b>CHAPTER 1 INTRODUCTION.....</b>	<b>1</b>
1.1 Introduction .....	1
1.2 Background.....	1
1.3 Problem Statement.....	4
1.4 Objectives .....	5
1.5 Scope of Studies .....	6
1.6 Thesis Organization.....	7
<b>CHAPTER 2 LITERATURE REVIEW.....</b>	<b>8</b>
2.1 Introduction .....	8
2.2 Properties of Zinc Oxide.....	8
2.2.1 Crystal Structure of ZnO.....	10
2.2.2 Electrical Properties of ZnO.....	13
2.2.3 Optical Properties of ZnO.....	15

2.2.4	Surface of ZnO .....	18
2.3	Growth of ZnO Nanostructure.....	20
2.3.1	Wet Oxidation.....	21
2.3.2	Hydrothermal.....	22
2.3.3	Chemical Bath Deposition.....	23
2.4	Growth Mechanism .....	24
2.5	Applications of ZnO.....	26
2.6	Laser .....	28
2.6.1	Laser Types.....	31
2.6.1(a)	Gas Laser .....	32
2.6.1(b)	Solid State Laser.....	33
2.6.1(c)	Semiconductor Laser .....	34
2.7	Random Laser.....	37
2.8	Review on ZnO based Random Laser.....	42
2.9	Review of insulating material on ZnO based devices.....	44
2.10	Metal-Semiconductor Contact.....	46
2.10.1	Ohmic Contact.....	47
2.10.2	Schottky Contact .....	52
2.10.2(a)	Schottky Barrier Height.....	56
2.10.2(b)	Current Transport in Schottky Contact.....	59
2.10.2(c)	Review of Schottky Contact on ZnO.....	61
<b>CHAPTER 3 METHODOLOGY.....</b>		<b>64</b>
3.1	Introduction .....	64

3.2	Preparation of Substrates .....	64
3.3	Growth of ZnO NRs on ITO Glass Substrate.....	66
3.3.1	Sputtering Process .....	66
3.3.2	Annealing .....	69
3.3.3	Chemical Bath Deposition.....	70
3.4	Characterization Tools.....	72
3.4.1	Field Effect Scanning Electron Microscopy and Energy Dispersive X-Ray Analysis.....	72
3.4.2	X-Ray Diffractometer .....	74
3.4.3	UV-Visible Spectroscop .....	77
3.4.4	Photoluminescence Spectroscopy.....	79
3.5	Fabrication of MIS Schottky diode.....	80
3.5.1	Current-Voltage Characterization.....	81
3.5.2	Electroluminescence Spectroscopy .....	82
3.6	Summary .....	84
	<b>CHAPTER 4 RESULTS AND DISCUSSIONS.....</b>	<b>86</b>
4.1	Introduction .....	86
4.2	Characterization of ZnO NRs.....	86
4.2.1	FESEM Analysis and EDX of ZnO NRs.....	86
4.2.2	X-Ray Diffraction Analysis .....	91
4.2.3	Photoluminescence Analysis .....	93
4.2.4	UV-Vis Analysis .....	95
4.3	Current-Voltage Measurement .....	98

4.4	Electroluminescence Analysis .....	108
4.5	Summary.....	115
<b>CHAPTER 5 CONCLUSION AND RECOMMENDATION.....</b>		<b>117</b>
5.1	Conclusion.....	117
5.2	Recommendation for Future Work.....	118
<b>REFERENCES.....</b>		<b>119</b>
<b>APPENDICES</b>		
<b>LIST OF PUBLICATIONS</b>		

## LIST OF TABLES

	<b>Page</b>
Table 2.1 Physical properties and parameter values of wurtzite ZnO [42]. . . . .	9
Table 2.2 Electron mobility of ZnO with different synthesis method. . . . .	14
Table 4.1 Diameter distribution of ZnO NRs. . . . .	90
Table 4.2 Analysis data for the ZnO NRs synthesized. . . . .	93
Table 4.3 The <i>I-V</i> parameters for each sample. . . . .	104
Table 4.4 Data based on existing literatures. . . . .	105
Table 4.5 The range of applied voltage for each region for each sample. . . . .	108
Table 4.6 Data of threshold current based on existing literatures. . . . .	111



## LIST OF FIGURES

	<b>Page</b>
Figure 2.1 Interpenetrating hexagonal closed-pack (hcp) structure.....	10
Figure 2.2 Crystal structure of ZnO: (a) cubic rocksalt (b) cubic zincblende, and (c) wurtzite [44].....	11
Figure 2.3 Hexagonal wurtzite structure of ZnO with lattice parameters [48].....	12
Figure 2.4 Excitons (a) Wannier excitons (b) Frenkel excitons [55].....	16
Figure 2.5 Typical room temperature photoluminescence spectrum of ZnO NRs deposited at 65 °C using linear sweep voltammetry technique [60] .....	18
Figure 2.6 Polar and nonpolar faces of ZnO along c-axis [61].....	19
Figure 2.7 Growth morphologies of 1-dimensional ZnO nanostructure [24].....	20
Figure 2.8 HMTA hindered the horizontal growth of ZnO by attaching themselves to the nonpolar surfaces of ZnO [96].....	26
Figure 2.9 Structure of laser. Mirror 1 is a high reflectance mirror while mirror 2 is a partially transparent mirror. Energy input to stimulate the atom to higher energy state. The atoms of higher energy state then relaxed to their ground state by spontaneous emission. The spontaneous emission are of random direction except the one on axis. The spontaneous emission on the axis will then caused a series of stimulated emission to generate laser [120].....	29
Figure 2.10 Schematic diagram of (a) induced absorption: electron absorbed	

photon of energy  $h\nu$  to move from lower energy state  $E_1$  to higher energy state  $E_2$  (b) spontaneous emission: electron relaxed from higher energy state  $E_2$  to lower energy state  $E_1$  by releasing photon of energy  $h\nu$  (c) stimulated emission: electron dropped from higher energy state  $E_2$  to lower energy state  $E_1$  by releasing photon of energy  $h\nu$  due to interaction with the incoming photon of energy  $h\nu$  [121].....31

Figure 2.11 Energy diagram of ruby laser. Blue and green light incident on ruby crystal excite the electron to excited state 2 and 3 respectively. Electron then relaxed to ground state by emitting red light after phonon emission to excited state 1.....34

Figure 2.12 Band diagram of semiconductor laser under forward bias [151].....36

Figure 2.13 Formation of random laser. Photons are scattered in the medium and followed a random path. When the scattered photons formed a closed loop, random laser is generated [159]. The black dots represent scatterer while the purple arrows represent photon's path.....38

Figure 2.14 (a) Localized mode (b) Extended mode [165].....40

Figure 2.15 (a) Thermionic emission (TE) for low concentration majority carriers, the carriers are thermally excited over the barrier (b) Thermionic field emission (TFE) for intermediate concentration majority carriers, the carriers are thermally excited

to an energy where the barrier is narrow enough for tunneling to occur (c) Field emission (FE) for high concentration majority carriers, the barrier is narrow enough at the bottom of conduction band such that carriers can tunnel through directly [200]. .....47

Figure 2.16 Energy band diagram of metal and n-type semiconductor before contact [121].  $\phi_m$  is the metal work function,  $\chi$  is the electron affinity of the semiconductor and  $\phi_s$  is the semiconductor work function. ....48

Figure 2.17 Energy band diagram of metal and n-type semiconductor after contact [121].  $\phi_{Bn}$  is the Schottky barrier height and  $\phi_n$  is the potential difference (magnitude) between  $E_c$  and  $E_F$  in n-type semiconductor.....49

Figure 2.18 Ideal energy band diagram of ohmic contact where  $E_c$  is conduction band energy while  $E_v$  is valence band energy when positive bias is applied on the metal [201].....50

Figure 2.19 Ideal energy band diagram of ohmic contact where  $E_c$  is conduction band energy while  $E_v$  is valence band energy when positive bias is applied on the semiconductor [201].....50

Figure 2.20 Energy band diagram of heavily doped n-type semiconductor for ohmic contact [121]. The electrons are tunneling through the barrier in both directions.....51

Figure 2.21 Ideal energy band diagram of n-type semiconductor and metal

	before contact [121]. $\phi_m$ is the metal work function, $\chi$ is the electron affinity of the semiconductor and $\phi_s$ is the semiconductor work function.....	52
Figure 2.22	Ideal energy band diagram of n-type semiconductor and metal after contact [121]. $\phi_{B0}$ is the ideal Schottky barrier height, $V_{bi}$ is the built-in potential barrier and $x_n$ is the width of depletion region.....	53
Figure 2.23	Ideal energy band diagram of metal and n-type semiconductor contact in forward biased [121]. The lowering value of $V_{bi}$ enable more electron to flow through.....	55
Figure 2.24	Ideal energy band diagram of metal and n-type semiconductor contact in reversed biased [121]. The increasing value of $V_{bi}$ alongside depletion region restricted the flow of electron.....	56
Figure 2.25	Image charge modeling of Schottky effect [121]. $x$ is distance of electron in semiconductor to metal surface.....	57
Figure 2.26	Energy band diagram of Schottky effect [121].....	58
Figure 2.27	Energy band diagram of current transport under forward biased [121]. $J_1$ represent current density from metal to semiconductor while $J_2$ represent current density from semiconductor to metal.....	61
Figure 3.1	Substrates after the cutting process.....	65
Figure 3.2	Sample preparations for ultrasonic bath.....	65
Figure 3.3	Sputtering model Auto HHV 500 Sputter Coater and schematic	

	diagram of sputtering process.....	68
Figure 3.4	Substrates after sputtering.....	68
Figure 3.5	Furnace of model Naber-Labotherm R70/9.....	69
Figure 3.6	Setup of CBD for ZnO NRs.....	71
Figure 3.7	(a) FESEM machine of model FEI Nova NanoSEM 450 (b) Schematic diagram of FESEM [239].....	73
Figure 3.8	XRD model of PANalytical X'pert PRO MRD PW3040.....	74
Figure 3.9	Bragg diffraction. [240] .....	75
Figure 3.10	Schematic diagram of XRD.....	76
Figure 3.11	UV-Vis spectroscopy of model Cary 5000 UV-Vis-NIR.....	78
Figure 3.12	The schematic diagram of the fabricated MIS device with Pd metal contact on top of SiO <sub>2</sub> insulating layer followed by ZnO NRs and ITO glass underneath ZnO nanorods.....	81
Figure 3.13	Schematic diagram of IV measurement.....	82
Figure 3.14	Schematic diagram of EL using Jaz Modular Sensing Suite.....	83
Figure 3.15	Flowchart of methodology in this project.....	85
Figure 4.1	Top view FESEM image of ZnO NRs.....	87
Figure 4.2	Cross-section FESEM image of the ZnO NRs.....	88
Figure 4.3	Bar chart of the number of NRs vs diameter of NRs.....	89
Figure 4.4	The EDX spectrum of ZnO NRs.....	91
Figure 4.5	Stack of XRD spectra of ZnO seed layer and ZnO NR grown by CBD.....	92
Figure 4.6	PL spectra from the ZnO NRs sample on ITO. ....	94

Figure 4.7	(a) Transmittance (b) Reflectance and (c) Absorbance spectra of ZnO NRs samples.....	95
Figure 4.8	Tauc Plot of 0.05 M ZnO NRs sample on ITO.....	97
Figure 4.9	Kubelka-Munk plot of 0.05M ZnO NRs sample on ITO.....	97
Figure 4.10	<i>I-V</i> characteristics of Pd/SiO <sub>2</sub> /ZnO nanorods MIS Schottky diode with different SiO <sub>2</sub> thickness in dark environment. The inset shows the <i>I-V</i> characteristics of Al/ZnO nanorods/ITO Ohmic contact.....	98
Figure 4.11	Fabricated Pd/SiO <sub>2</sub> /ZnO MIS Schottky diode.....	99
Figure 4.12	Graph of ln I vs V for all samples.....	101
Figure 4.13	$\frac{dV}{d(\ln I)}$ vs <i>I</i> plots of fabricated devices (a) 50 nm (b) 55 nm (c) 65 nm and (d) 70 nm at room temperature.....	103
Figure 4.14	Log-log graph for Pd/SiO <sub>2</sub> /ZnO MIS Schottky diode samples with the increasing SiO <sub>2</sub> thickness, R represents the region of the sample.....	106
Figure 4.15	(a) EL spectra for each fabricated device at their corresponding threshold current (b) Graph of threshold current vs thickness of SiO <sub>2</sub> (c) emission from the fabricated Pd/SiO <sub>2</sub> /ZnO device.....	109
Figure 4.16	EL spectra of 55 nm sample at different current input.....	112
Figure 4.17	Schematic diagrams for the energy band structures at forward Biased.....	113

## LIST OF SYMBOLS

$a_0$	Lattice constant in a-axis for bulk material
$c_0$	Lattice constant in c-axis for bulk material
$T$	Temperature
$a, c$	Lattice constant
$U$	Electric potential energy
$e$	Charge of an electron
$\epsilon_0$	Vacuum permittivity
$\epsilon$	Dielectric constant
$r$	Distance between hole and electron
$\mu$	Reduced mass
$m_e^*$	Effective mass of electron
$m_h^*$	Effective mass of hole
$E_n$	Energy of exciton
$E_g$	Band gap energy
$\hbar$	Reduced planck's constant
eV	Electron volt
$E_{Fn}$	Quasi-Fermi level of electron
$E_{Fp}$	Quasi-Fermi level of hole
$h$	Planck's constant
$\nu$	Frequency of photon
$l$	Transport mean free path

$L$	Length of material size
$\lambda$	Wavelength
$\phi_m$	Metal work function
$\chi$	Electron affinity
$\phi_s$	Semiconductor work function
$\phi_{Bn}$	Schottky barrier height
$\phi_{B0}$	Ideal Schottky barrier height
$V_{bi}$	Built-in potential barrier
$x_n$	Width of depletion region
$E_F$	Fermi level
$E_c$	Conduction band energy level
$\phi_n$	Potential difference between $E_c$ And $E_F$
$V_a$	Applied voltage
$V_R$	Reversed biased voltage
$\epsilon_s$	Permittivity of semiconductor
$N_d$	Density of donor atoms
$E$	Electric field
$\phi$	Potential
$x$	Distance of electron in semiconductor to metal surface
$\phi_0$	Surface potential
$J_0, J_1, J_2$	Current density
$k$	Boltzmann constant
$A^*$	Effective Richardson constant



$d_{hkl}$	Interplanar spacing
$D$	Crystallite size
$\beta$	Full width half maximum in radians
$hkl$	Miller indices
$\varepsilon$	Lattice strain
$\alpha$	Absorption coefficient
$V$	Voltage
$I_0$	Saturation current
$A$	Diode area
$R_s$	Series resistance
$I$	Current

## LIST OF ABBREVIATIONS

Ar	Argon
CB	Conduction Band
CBD	Chemical Bath Deposition
CSP	Chemical Spray Pyrolysis
CVD	Chemical Vapor Deposition
CXA	Computer X-Ray Analyser
DC	Direct Current
DLE	Deep Level Emission
EDX	Energy-Dispersive X-Ray
EL	Electroluminescence
FE	Field Emission
FESEM	Field Emission Scanning Electron Microscopy
GaAs	Gallium Arsenide
GaN	Gallium Nitride
GaSb	Gallium Antimonide
HMTA	Hexamethylenetetramine
ICSD	Inorganic Crystal Structure Database
InAs	Indium Arsenide
ITO	Indium Tin Oxide
IV	Current-Voltage
LED	Light Emitting Diode
MBE	Molecular Beam Epitaxy

MIS	Metal-Insulator-Semiconductor
MOCVD	Metal Organic Chemical Vapor Deposition
MOS	Metal-Oxide-Semiconductor
MS	Metal-Semiconductor
NaCl	Sodium Chloride
NBE	Near Band Edge
NIR	Near Infrared
NRs	Nanorods
O	Oxygen
Pb	Graphene
Pd	Palladium
PL	Photoluminescence
PLD	Pulsed Laser Deposition
PVD	Physical Vapor Deposition
RF	Radio Frequency
SBH	Schottky Barrier Height
SEM	Scanning Electron Microscopy
SiO <sub>2</sub>	Silicon Dioxide
TE	Thermionic Emission
TEM	Transmission Electron Microscopy
TFE	Thermionic Field Emission
UV	Ultraviolet
UV-Vis	Ultraviolet-Visible

VB	Valence Band
XRD	X-Ray Diffraction
Zn	Zinc
ZnO	Zinc Oxide

## **LIST OF APPENDICES**

APPENDIX A XRD – Database Zinc Oxide

APPENDIX B XRD – Database Indium Tin Oxide

# **PERTUMBUHAN DAN PENCIRIAN PD/SIO<sub>2</sub>/NANOROD ZNO UNTUK PERANTI LASER RAWAK DIPAM SECARA ELEKTRIK**

## **ABSTRAK**

ZnO muncul sebagai satu bahan semikonduktor yang mempunyai potensi dalam peranti optik, sentuhan ohmik telus, filem nipis telus dan transistor heterostruktur, penderia kimia/bio dan piezotransduser disebabkan oleh sifatnya seperti tenaga pengikat eksiton yang tinggi dan tenaga jurang jalur langsung yang besar. Banyak kertas penyelidikan telah diterbitkan mengenai ZnO atas keupayaannya untuk menghasilkan nanostruktur yang berbeza. Nanostruktur ZnO boleh dihasilkan dalam pelbagai bentuk dengan parameter pertumbuhan yang sesuai. Nanorod ZnO telah dipilih sebagai sasaran penyelidikan dalam kajian ini kerana nisbah permukaan kepada isipadu yang tinggi, dan kemudahan proses fabrikasi. Di antara semua teknik penumbuhan, pemendapan rendaman kimia (CBD) merupakan satu teknik yang mudah, kos rendah dan mesra alam. Proses CBD dijalankan selepas lapisan benih telah dimendapkan di atas substrat kaca ITO melalui teknik percikan RF. Kaca ITO dipilih sebagai substrat kerana lutsinar dan kekonduksian elektrik yang baik. Morfologi nanorod ZnO yang dihasilkan dari CBD dikawal dengan mengekalkan parameter penumbuhan. Pembolehubah ditetapkan pada 0.05 M kepekatan larutan prekursor, tempoh 3 jam dan pada suhu 96 °C. Pencirian ZnO nanorod diperiksa melalui analisis Ultraungu-Cahaya nampak (UV-Vis), Pembelauan X-Ray (XRD), Mikroskop Imbasan Elektron Pancaran Medan (FESEM), Sebaran Tenaga X-Ray (EDX), dan Pendarkilau (PL). Data yang diperoleh daripada pencirian di atas

adalah dalam julat yang munasabah selepas dibandingkan dengan kajian sedia ada. Laser rawak dipam secara elektrik diketahui sangat mencabar kepada para penyelidik sekian lama disebabkan kesukaran untuk fabrikasi. Jadi, untuk mengetahui faktor yang mempengaruhi realisasi laser rawak yang dipam secara elektrik, penyiasatan ke atas peranti laser rawak MIS adalah diperlukan. Untuk menghasilkan peranti MIS, lapisan penebat SiO<sub>2</sub> dipercik di atas nanorod ZnO oleh percikan Arus Terus (DC) diikuti oleh logam Pd. Ketebalan lapisan SiO<sub>2</sub> yang berbeza (50 nm, 55 nm, 65 nm, dan 70 nm) dimendapkan bagi meneroka ciri-ciri *I-V* serta keadaan lasing. Peranti MIS yang difabrikasi kemudiannya digunakan untuk menjana laser rawak melalui pengepaman elektrik. Melalui pencirian *I-V*, semua sampel menunjukkan ciri-ciri Schottky yang baik. Ketinggian hadangan Schottky, rintangan siri dan arus ambang didapati meningkat apabila ketebalan SiO<sub>2</sub> meningkat. Walaupun kesemuanya menunjukkan ciri-ciri Schottky yang baik, sampel 55 nm didapati adalah yang terbaik. Oleh itu, sampel 55 nm diuji lagi untuk EL pada input arus yang berbeza (27 mA, 29 mA, 32 mA, 35 mA, 38 mA, 42 mA dan 45 mA). Berdasarkan spectra EL, peralihan daripada spektra LED kepada spektra laser rawak berlaku pada 32 mA. Melempi 32 mA pancaran laser rawak didapati berterusan dengan peningkatan pancaran spontan. Kesimpulannya, struktur peranti seperti ini berpotensi untuk digunakan sebagai peranti laser rawak bagi aplikasi optoelektronik termaju.

# **GROWTH AND CHARACTERIZATION OF PD/SiO<sub>2</sub>/ZNO NANORODS FOR ELECTRICALLY PUMPED RANDOM LASER**

## **ABSTRACT**

ZnO appeared to be a promising semiconductor material in optical devices, transparent ohmic contacts, transparent thin film and heterostructure transistors, chemical/bio sensors, and piezotransducers owing to its properties such as high exciton binding energy and large direct band gap. Many research papers have been generated based on the studies of ZnO due to its ability to grow as different type of nanostructures. ZnO nanostructures can be prepared in many different shapes by customizing the growth parameters. ZnO nanorods has been chosen to be the research target in this work owing to its high surface to volume ratio, and simplicity to fabricate. Among all the growth techniques, Chemical Bath Deposition (CBD) stand out to be an easy and low cost technique. CBD process is carried out after seed layer is deposited on top of the ITO glass substrate via sputtering technique. ITO glass is chosen to be the substrate due to its goods transparency and electrical conductivity. Morphologies of ZnO nanorods grown by CBD is fixed by maintaining the growth parameters. The characteristics of ZnO nanorods is examined through Ultraviolet-Visible (UV-Vis), X-Ray Diffraction (XRD), Field Emission Scanning Electron Microscope (FESEM), energy-dispersive X-ray (EDX) and photoluminescence (PL) measurement. The data obtained from the above characterization are within reasonable range after comparing to existing literatures. Electrically pumped random laser has been haunting the researchers for years due to its difficulty to fabricate.



Thus, to have an insight on the factor that is influencing the realization of electrically pumped random laser, an investigation on MIS random laser devices is required. To fabricate MIS devices, SiO<sub>2</sub> insulating layer is sputtered on top of ZnO nanorods by DC sputtering followed by Pd metal. Different thickness of SiO<sub>2</sub> layer (50 nm, 55 nm, 65 nm and 70 nm) are deposited to explore *I-V* characteristics as well as lasing behavior. The MIS device fabricated is then used for generating random laser through electrical pumping. Based upon the *I-V* characterization, all samples exhibit good Schottky behavior. The Schottky barrier height, series resistance and threshold current increased in magnitude as the SiO<sub>2</sub> thickness increased. Although all samples showed good Schottky behavior, the 55 nm sample stands out to be the best among them. The 55 nm sample is further tested for EL at different current input (27 mA, 29 mA, 32 mA, 35 mA, 38 mA, 42 mA, and 45 mA) as it is considered the best sample among others. Based on the EL spectra the transition from LED spectra to random lasing spectra occurs at 32 mA. Beyond 32 mA the lasing characteristics persist with an increasing in spontaneous emission. It can be concluded that this kind of device structure has the potential to be utilised as random laser for applications in advanced optoelectronics.

# CHAPTER 1

## INTRODUCTION

### 1.1 Introduction

In this chapter, background of the thesis will be presented, followed by the problem statements, research objectives, as well as the scope of the study. At the end, this chapter will be concluded by the thesis organization section.

### 1.2 Background

Semiconductors have been a very important element in the field of optics and electronics throughout the century. Successful research in the field of semiconductors has improved the technologies of mankind and brought convenience to our life. A lot of research has been done on various types of semiconductors such as silicon [1], gallium nitride [2][3], and gallium arsenide [4] to explore for a new technology. Semiconductors have high demand across the world as they can be used in sensor [5], [6], solar cell [7][8], light emitting diode (LED) [9][10] and laser [11] application. With the rise of nanotechnology in recent years, semiconductors have experienced a great leap in their applications. Nanotechnology was first coined by physicist Richard Feynman, which also the Nobel Prize winner in 1959 [12]. Nanotechnology can be defined as a technology concerning processes which are relevant to physics, chemistry and biology taking place at a length scale of one divided by 100 million of a meter [13]. It is important in the current era because it could make the technology become relatively cheap, safe, and clean [14]. Nanotechnology also has attracted numerous attractions from many scientists due to its

applications in electronic devices [15], optical devices [12] and biotechnology [16]. Because of this, many developed countries have viewed nanotechnology as the future. Nanotechnology in semiconductor field involved the creation of nanostructure of certain material such as zinc oxide (ZnO) [17][18], gallium nitride (GaN) [3][19] and zinc hydroxide ( $\text{Zn}(\text{OH})_2$ ) [20]. Nanostructures can be classified into 4 groups which are 0-dimensional nanomaterial (0D), 1-dimensional nanomaterial (1D), 2-dimensional nanomaterial (2D) and 3-dimensional nanomaterial (3D). 0-dimensional nanomaterials (0D) are defined as nanomaterials in which all their dimensions are measured within nanoscale. Some examples of 0D nanomaterials are quantum dots and nanoparticles [21][22]. 1-dimensional nanomaterials (1D) included nanotubes, nanobelts and nanorods. Recently, 1D nanomaterials have stirred up a lot of interest due to their possible and integral application in photonics and electronics devices in the future. 2-dimensional nanomaterials are defined as having two dimensions outside of the nanometric size range [22]. Quantum wells and nanowall both are considered as 2D nanostructures [23][24]. 3-dimensional nanomaterials are materials that are not confined to the nano scale in any dimension. They are usually a bulk material [21]. 3D nanostructure included nanocoils, nanocones and nanoflowers [22]. All four of these different groups of nanostructures have their own application in fuel cells, supercapacitors and Li-ion batteries [22].

Among many semiconductors such as GaN, gallium arsenide (GaAs) and graphene, ZnO has successfully attracted many researchers due to its unique properties. ZnO has demonstrated its application in LED [25-27], transistor [28], lasers [27], and even solar cell [29]. ZnO does not limit its application only in electronic and photonic field, but it extends its application further to cosmetics [30] and personal care products [31]. As

mentioned above, nanomaterials can form many kinds of structure based on their dimensionality. In this work, the focus would be on 1D nanostructures. ZnO can form many different morphologies of 1D nanostructures such as nanobelts, nanotubes and nanorods by using different growing parameters. Each of these nanostructures have unique properties and applications in optics and electronics devices. Much research has been performed on 1D ZnO nanostructure given its promising potential applications [17][32][33]. ZnO nanorods, a 1D nanostructures has been given high attention due to its high surface to volume ratio and simplicity to shape [34]. Hence, ZnO nanorods has been selected to be the investigation target in this work.

The fabrications of ZnO nanorods can be performed in many different techniques such as chemical vapor deposition (CVD) [35], pulsed laser deposition (PLD) [36], molecular beam epitaxy (MBE) [37], hydrothermal method [24] and chemical bath deposition (CBD) [17]. From the numerous growing techniques, CBD technique has been chosen in this project. What distinguished CBD from the other growing techniques is its ability to reproduce, considerably lower cost, simplicity, low temperature and only required normal atmospheric pressure [24]. The discussion on different growth techniques of ZnO nanorods including CBD will be further discussed in Chapter 2.

Due to the demand of lasers in many fields, various types of lasers have been invented and developed. For example, gas laser, solid state laser, semiconductor laser and dye laser. Nevertheless, the lasers mentioned above cannot cover the fact that a directional and coherent light will generate speckle which is an unwanted phenomenon. Thus, these types of lasers cannot be an ideal lighting source. The creation of random laser reduces the speckle pattern and further consolidates itself as an ideal candidate in lighting

applications. Random laser could be generated via scattering in dye particles, nanoparticles and even nanorods without the need of a Fabry-Perot cavity. In a random and disorder system, a scattered photon could be traced back to its original position forming a closed loop. When the gain inside the closed loop exceeds the loss, laser emission will be generated. To the best of our knowledge, electrically pumped random laser with ZnO nanorods synthesized by CBD is a relatively young field. Thus, performance of electrically pumped random laser will be investigated alongside different thickness of SiO<sub>2</sub> grown on ZnO nanorods as the variables.

### **1.3 Problem Statement**

1. The fabrication of ZnO nanorods based devices with high crystal quality, optical and electrical properties often associated with synthesise method that required high cost, time consuming and even extreme condition such as Chemical Vapor Deposition (CVD) and Pulsed Laser Deposition (PLD). To overcome these issues, a relatively new method- Chemical Bath Deposition known as CBD which has the advantages of low cost and simple to produce is selected as our synthezised method. Thus, a study on the various properties of ZnO nanorods synthesized is required.

2. Electrically pumped random laser is a relatively new field when compared to optically pumped random laser. From literature, we can know that electrically pumped random laser has faced many obstacles and offered a lot of challenges to fabricate. Thus, in order to have an insight on the element that is affecting the realization of electrically pumped random laser, an investigation of different MIS random laser devices is required.

A study on the different metal-insulator-semiconductor interface can ease the achievement of electrically pumped random laser in the future.

3. The lasing quality of random laser can be varying depends on its material and even its device structure. Realization of high quality electrically pumped random lasing from this sample would provide a broader avenue in making random laser device for practical application.

#### **1.4 Objectives**

The objectives of this research are:

1. To investigate the characteristics of ZnO nanorods synthesized by CBD for the development of Pd/SiO<sub>2</sub>/ZnO nanorods device.
2. To access the electrical properties of Pd/SiO<sub>2</sub>/ZnO nanorods MIS device.
3. To evaluate the lasing performance of Pd/SiO<sub>2</sub>/ZnO nanorods random laser devices.

## 1.5 Scope of Studies

The methodology of this research will involve synthesizing of ZnO nanorods by CBD on seeded ITO coated glass substrates, followed by morphological, structural, and optical characterization through Field Emission Scanning Electron Microscope (FESEM), energy-dispersive X-ray (EDX), X-Ray Diffraction (XRD), UV-Visible (UV-Vis), and photoluminescence (PL) measurements, respectively. Later, random laser devices based upon the ZnO nanorods will be fabricated by depositing different thickness of SiO<sub>2</sub> layer (50 nm, 55 nm, 65 nm, and 70 nm) on ZnO NRs followed by a layer of Pd metal. Electrical characterization of MIS diode of different SiO<sub>2</sub> thickness using *I-V* characterization will be carried out. And the final part is the performance evaluation of the complete device using EL spectra measurement.

## **1.6 Thesis Organization**

This thesis is divided into several chapters, based on the following:

Chapter 1 states the introduction, background, problem statement, research objectives, scope of studies and the thesis organization.

Chapter 2 provides the literature review from several books, journals, and papers. This chapter describes the properties of ZnO, CBD growth mechanism, Schottky contact, MIS/MS junction as well as random laser devices which related to this project.

Chapter 3 describes the methodology and the equipments used in this work. The type of characterizations and the basic working principle of the equipment used are also explained.

Chapter 4 shows the results and discussion. The morphological, structural and optical characterizations of the ZnO NRs are presented here. The electrical characterization of the fabricated MIS devices is also presented here. Finally, this chapter concludes with the presentation of EL of all devices.

Chapter 5 provides the conclusion of this thesis. All the results are summarized and recommendations for future work are also presented in this chapter.



## **CHAPTER 2**

### **LITERATURE REVIEW**

#### **2.1 Introduction**

In this chapter, the discussion will cover the detail on backgrounds, basic properties and structural of ZnO. Several types of ZnO NRs synthesis techniques will also be included. The CBD synthesized technique, employed in this work will also be described in detail. For the device, introduction on the basic principle of metal-semiconductor junctions will be presented. Moreover, the discussion will also cover the background, basic principles, type of lasers, along with random laser devices. Overall, contribution of the related literatures had provided a significant insight and knowledge to further understand the project.

#### **2.2 Properties of Zinc Oxide**

ZnO is a II-VI inorganic semiconductor with a direct and wide bandgap ( $\approx 3.36$  eV) [18][38][39] which would enable it to operate at high voltage, frequency and power level. It also exhibits some other unique properties such as large exciton binding energy ( $= 60$  meV) [38][39] at room temperature which would guaranteed an efficient excitonic emission. Furthermore, a high electron mobility in ZnO would ensure a better device performance, since the electron can move quickly through the semiconductor. Since it is transparent to visible light [40], and high in thermal conductivity, it would also enable high efficiency of heat removal during operation [41]. Due to these outstanding features, ZnO has become a promising semiconductor candidate in optoelectronics, transparent

electronics, spintronic devices, and various sensor application such as humidity sensor, and gas sensor. ZnO is insoluble in water but dissolves in most acid as well as alkali. It is notable that ZnO reacts vigorously with aluminium and magnesium powder. Moreover, ZnO exhibits a high melting point and high heat capacity. The table below shows some physical properties of wurtzite ZnO.

Table 2.1: Physical properties and parameter values of wurtzite ZnO [42].

Properties	Value
$a_0$ (T = 300 K)	0.32469 nm
$c_0$ (T = 300 K)	0.52069 nm
Density	5.606 g/cm <sup>3</sup>
Melting point	2248 K
Relative dielectric constant	8.66
Band Gap	3.4 eV direct
Intrinsic carrier concentration	$< 10^6$ cm <sup>-3</sup>
Exciton binding energy	60 meV
Electron effective mass	0.24
Electron mobility (T=300K)	200 cm <sup>2</sup> /V s
Hole effective mass	0.59
Hole mobility (T=300K)	5-50 cm <sup>2</sup> /V s

### 2.2.1 Crystal Structure of ZnO

In ZnO crystal, the bonding between Zn cation and O anion is a mixture of ionic and covalent since the difference in electronegativity is higher compared to traditional covalent bond, but lower compared to ionic bond. The electronegativity in ZnO is 1.79 [43]. The crystal of ZnO can be viewed as two interpenetrating hexagonal closed-pack (hcp) structures. Figure 2.1 represents a better illustration of ZnO crystal structure.

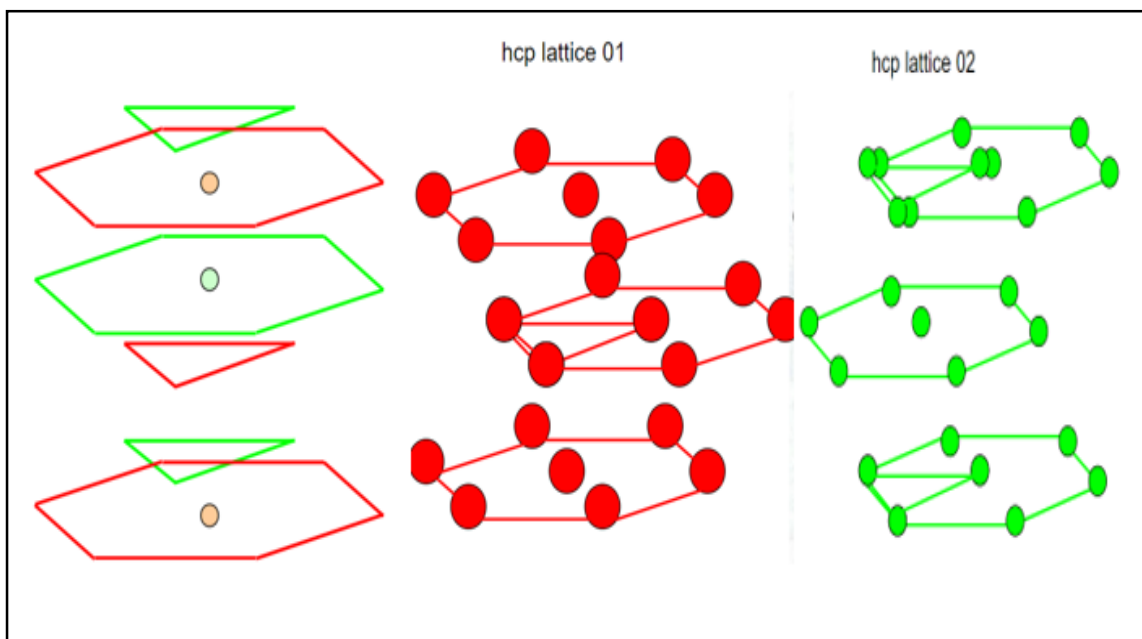


Figure 2.1: Interpenetrating hexagonal closed-pack (hcp) structure.

This type of structure is commonly referred to as the wurtzite crystal structure. ZnO can form three types of crystal structure namely hexagonal wurtzite, cubic rocksalt (NaCl) and cubic zincblende. Figure 2.2 shows three different crystal structures of ZnO.

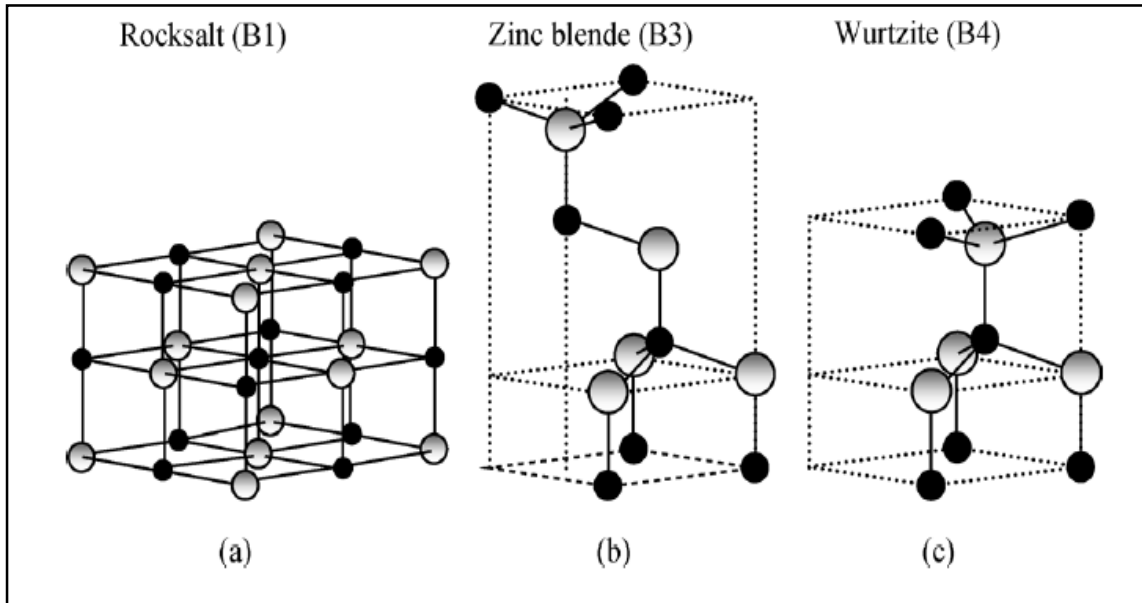


Figure 2.2: Crystal structure of ZnO: (a) cubic rocksalt (b) cubic zincblende, and (c) wurtzite [44].

Under ambient temperature and pressure, the most common crystal structure of ZnO is wurtzite since it is more stable thermodynamically. The cubic zincblende structure can only hold its stability by growing on a substrate with a cubic lattice structure, while the cubic rocksalt (NaCl) form can only be acquired at high pressure, which is around 10 GPa [44]. The reason for this is that high pressure can cause reduction in the lattice parameters which in turn causes the bonding between Zn ion and O ion to prefer ionic behavior more than covalent [44]. Inside the wurtzite crystal structure, Zn cation and O anion bond together in a tetrahedral geometry. This means each Zn cation is surrounded by four O anions at the corner of tetrahedral and vice versa. The unit cell of hexagonal wurtzite contains four atoms and does not possess a central symmetry structure due to the tetrahedral coordination of ZnO, and therefore it exhibits properties of piezoelectric [42][45]. The hexagonal wurtzite structure of ZnO has two lattice parameters,  $a$  and  $c$ .

The value of  $a$  at ambient conditions is approximately 0.32469 nm while the value of  $c$  is 0.52069 nm. For an ideal hexagonal wurtzite, the ratio of  $c/a$  is 1.633 [44], while for ZnO hexagonal wurtzite the value is in the range of 1.593-1.603 [46]. The difference in value is mainly due to the lattice parameters are affected by several factors such as excess of free-carriers, high concentration of point and extended defects and external stresses [47]. Figure 2.3 shows the hexagonal wurtzite structure of ZnO with lattice parameters.

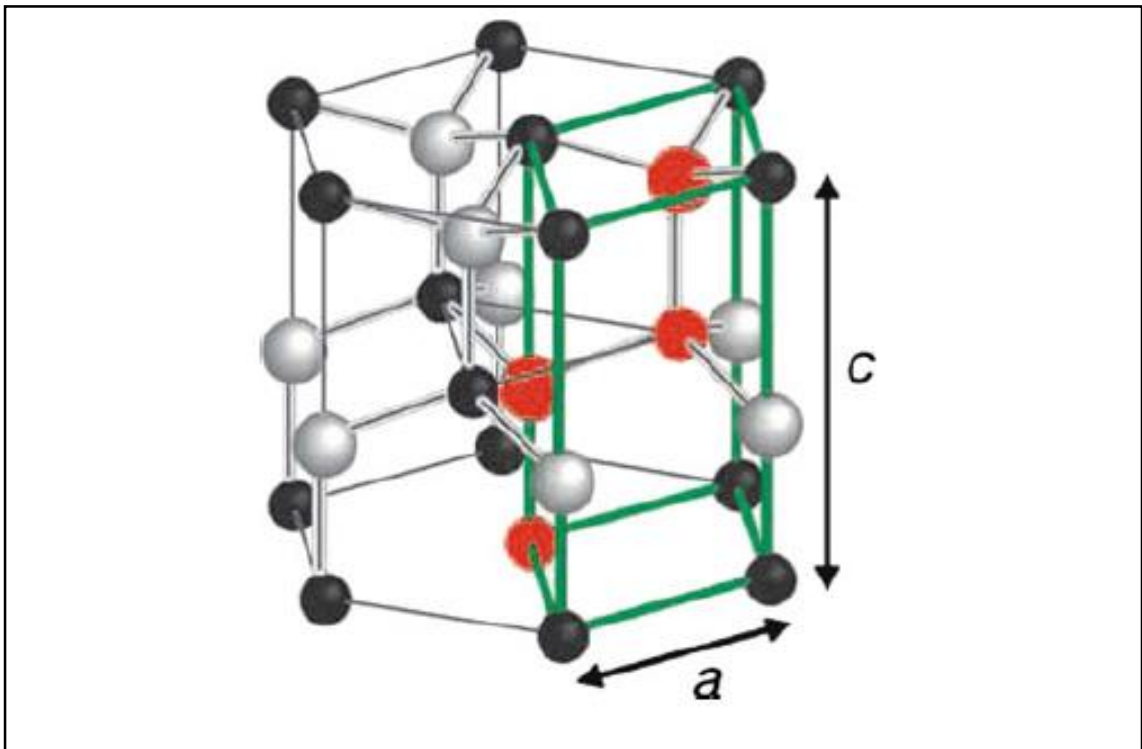


Figure 2.3: Hexagonal wurtzite structure of ZnO with lattice parameters [48].

### 2.2.2 Electrical properties of ZnO

As previously mentioned, ZnO has a wide and direct bandgap of 3.36 eV at room temperature, and high exciton binding energy at 60 meV. Additionally, ZnO is a natural n-type semiconductor material. This means that even for an undoped ZnO, it will always have the n-type property. Previously this n-type behavior of ZnO was widely believed to be due to native defects such as zinc interstitials and oxygen vacancies [49]. However, with the advance of technology, it has shown that this theory is not entirely correct since oxygen vacancies behave as deep donors, and thus cannot contribute to the electron to the conduction band [24][41][50]. While for zinc interstitials, although it always acts as a shallow donor it cannot be the origin of n-type conductivity since they will be present in very low concentrations in n-type ZnO [50]. Therefore, the n-type conductivity can only be caused by unintentionally incorporating hydrogen during the synthesis of ZnO. Further studies have been performed and confirmed that hydrogen acts as a shallow donor and it is the main reason for the natural n-type behavior [50]. One of the advantages of ZnO compared to other semiconductor materials is its high electron mobility. However, the electron mobility of ZnO is dependent on the synthesis method according to Ozgur et al. [44]. Table 2.2 compares the electron mobility of ZnO from variety of synthesis methods.

Table 2.2: Electron mobility of ZnO from different synthesis method [44].

Sample	Electron mobility ( $\text{cm}^2 \text{V}^{-1} \text{s}^{-1}$ )
Bulk ZnO grown by vapor-phase transport method	205
Bulk ZnO grown by pressurized melt method	131 (296 K)
	298 (77 K)
Bulk ZnO grown by hydrothermal method	200
ZnO thin film on <i>c</i> -plane sapphire substrates grown by PLD	155
ZnO thin films on <i>c</i> -plane sapphire grown by MBE	130
ZnO thin films grown on <i>a</i> -plane sapphire by MBE	120

Research work to obtain p-type doping of ZnO has been proven to post a difficult challenge because ZnO tends to turn into n-type material, and there is less material that can act as a shallow acceptor in ZnO [41]. If p-type doping ZnO could be achieved easily, it would provide a great leap in the field of semiconductors, especially in the application of laser and light emitting diode. For many years, many researchers have obtained p-type doping of ZnO [51][52][53] in their work, but reliability and ability to reproduce and replicate it is still a big concern.

### 2.2.3 Optical properties of ZnO

As aforementioned earlier, wide and direct bandgap of 3.36 eV with high exciton binding energy of 60 meV at room temperature, would enable ZnO to become a suitable and promising semiconductor material for blue/UV range photonics devices such as photodetectors, LED, and blue/UV lasers diode. Usually, the high exciton binding energy is often paid much attention since it is an integral part of determining the optical properties of the material. This is also the main reason why ZnO has become a favorable candidate for exciton-based devices. The high exciton binding energy ensures the exciton will not just dissociate into free electron and hole by thermal energy at room temperature since these excitons exhibit high thermal stability at room temperature.

In order to elucidate the optical properties of ZnO, the concept of exciton needs to be understood first. There exist two types of excitons, mainly Frenkel exciton which represent a small radius exciton and Wannier exciton, a large radius exciton. Frenkel exciton is a tightly bound exciton and localized on a single atom. They occur in molecular crystal and alkali halides [54][55]. On the other hand, Wannier exciton is a weakly bound exciton. They spread over many lattice constants and can move freely inside the material. This type of exciton can be found in semiconductors [54]. For ZnO, the focus will mainly be given on Wannier exciton. Figure 2.4 illustrates two types of excitons.



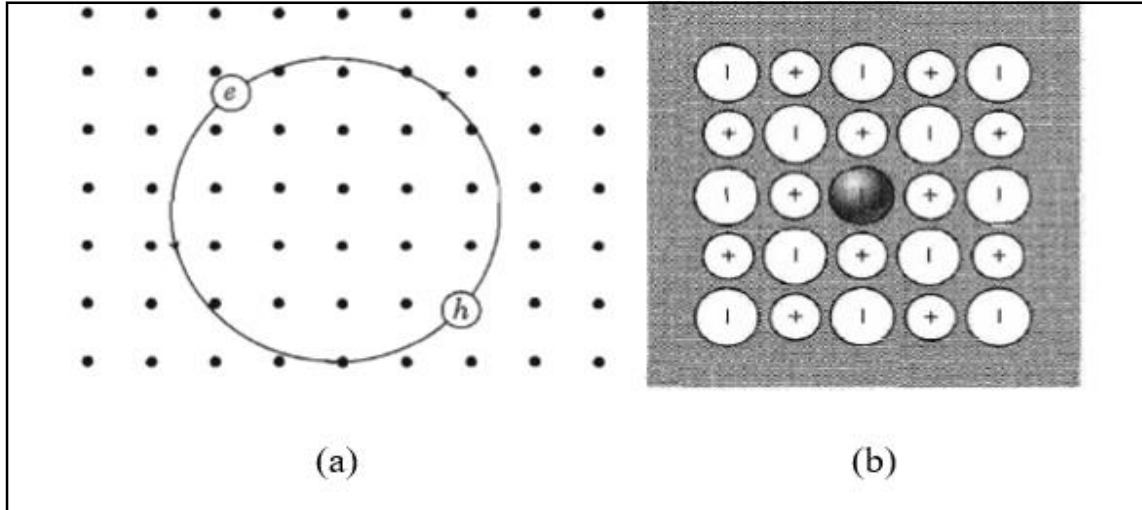


Figure 2.4: Illustration of excitons, (a) Wannier excitons, and (b) Frenkel excitons [55].

An exciton consists of an electron and a hole revolve around their center of mass. The attraction force between an electron and hole bound them together and the electric potential energy can be written as,

$$U(r) = -\frac{e^2}{4\pi \epsilon_0 \epsilon r} \quad (2.1)$$

where,  $e$  is the charge of an electron,  $\epsilon_0$  is the vacuum permittivity,  $\epsilon$  represents appropriate dielectric constant and  $r$  is the distance between hole and electron. If electron and hole were to merge into one particle by tuning their effective mass, then exciton can be analogous to hydrogen atom. The reduced mass,  $\mu$  can be written as,

$$\frac{1}{\mu} = \frac{1}{m_e^*} + \frac{1}{m_h^*} \quad (2.2)$$

where  $m_e^*$  is the effective mass of electron and  $m_h^*$  is the effective mass of hole. Since exciton is analogous to a hydrogen atom therefore its energy can be written by modifying the Rydberg equation for hydrogen atom,

$$E_n = E_g - \frac{\mu e^4}{2\hbar^2 \epsilon^2 n^2} \quad (2.3)$$

where,  $E_n$  is the energy of exciton at  $n$  level,  $E_g$  is the band gap energy,  $\hbar$  is the reduced Planck's constant and  $n$  is the principal quantum number of exciton. The exciton binding energy corresponds to the Equation 2.3 by setting the  $n$  value to the ground state of exciton which is 1. Although exciton is unstable with respect to their final recombination, they stable only if their binding energy is higher than the phonon energy. This indirectly indicates that exciton could only exist at low temperatures.

A classic PL spectrum of ZnO at ambient condition consists of a high and narrow peak of UV photon emission and a lower and wider peak of visible light emission. This result has been shown by many researchers [56][57]. The source of UV region emission is widely believed to be the recombination of exciton although recombination of free electron and hole could occurs as well. According to the work of M. Al Suleiman et al. [58], the PL intensity of ZnO nanorod is higher than bulk ZnO when compared at room temperature. They also stated that the longer the nanorod length the higher the PL intensity. There are several theories revolve around the origin of visible light emission such as impurities of copper ions, oxygen vacancies, zinc vacancies, zinc interstitials and oxygen interstitials [24][59]. From the works of several researchers, zinc vacancies show the strongest evidence as the source of green luminescence and is widely believed to be so. Nevertheless, the origin of visible spectrum is still currently under debate. Figure 2.5 below shows the typical ZnO PL luminescence graph.

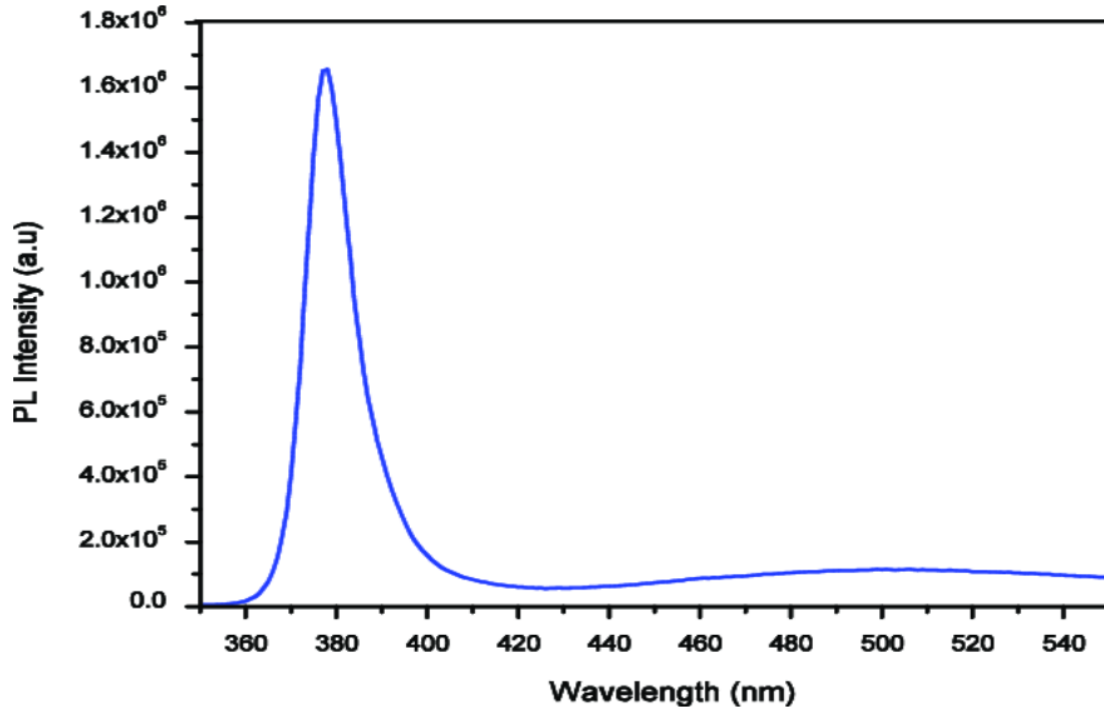


Figure 2.5: Typical room temperature photoluminescence spectrum of ZnO NRs deposited at 65 °C using linear sweep voltammetry technique [60].

#### 2.2.4 Surface of ZnO

It is well known that the surface of ZnO plays an integral part in determining its application's performance due to high surface to volume ratio [34]. For wurtzite ZnO crystal structure, there exists two polar surfaces and six non-polar surfaces [61] as shown in Figure 2.6. The non-polar surfaces exhibit no dipole because the surface contains the same amount of Zn and O atoms. The two polar surfaces are mainly (0001) Zn terminate face and (000 $\bar{1}$ ) O terminate faces. The reason for their polarity is because a single type of terminated atom resides on the surface [62]. These two surfaces exhibit their own dipole moment with Zn terminate surface being positive charged and O terminate surface being negative charged. (0001) Zn terminate face has a dipole moment pointing outward while

(000 $\bar{1}$ ) O terminate face has dipole moment pointing inward [63]. It has been stated by the author of [64] that the polar surface has higher surface energy than the nonpolar (100) and (110) surface. It has been shown experimentally that the (0001) surface is more active than (000 $\bar{1}$ ) surface in an environment with high oxygen levels as the surface energy of (0001) is higher [34]. In other word, the oxygen terminate surface is more stable in the above condition. According to the work of S. Akhter and coworkers, various compounds were adsorbed onto the surfaces of ZnO (including non-polar and polar surface) such as methanol, water, formic acid, and formaldehyde [63]. This indirectly implies that ZnO can act as a gas sensor. The ZnO's surface polarity could influence many features with one of it being the morphologies of nanostructure grown [61]. Other authors have successfully altered ZnO nanorod to nanotube by engineer the surface energy of ZnO nanorod [61].

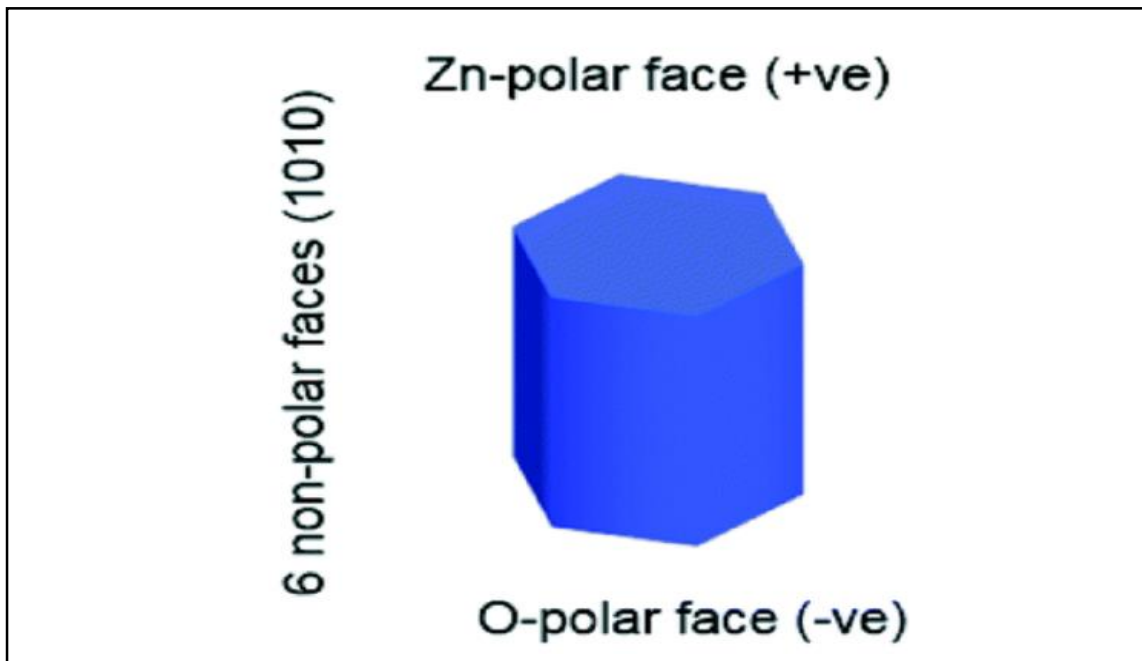


Figure 2.6: Polar and nonpolar faces of ZnO along *c*-axis [61].

### 2.3 Growth of ZnO nanostructure

As stated earlier, ZnO can form various morphologies such as nanoflower [22], nanorods [34], nanowalls [23][24] and nanobelts [32] depending on its growth condition. Figure 2.7 shows different growth morphologies of 1-dimensional ZnO nanostructure. Many techniques have been employed to synthesis ZnO nanostructure on a substrate. Different growing methods provide its own advantages and disadvantages. The techniques of synthesis ZnO nanostructure included hydrothermal method [24], PLD [36], CVD [35], CBD [17] and many more. This section will discuss the various growing methods of ZnO nanostructure.

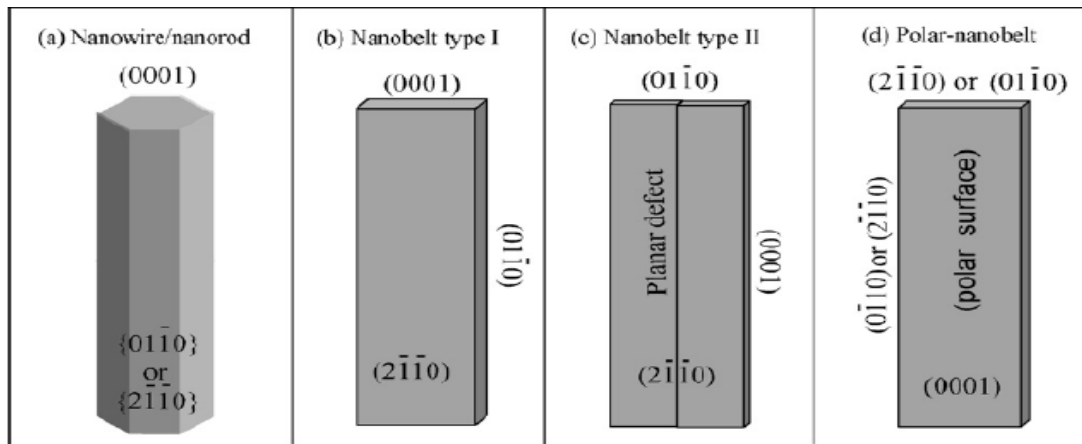


Figure 2.7: Growth morphologies of 1-dimensional ZnO nanostructure [24].

### 2.3.1 Wet Oxidation

Different types of ZnO nanostructures such as nanowires, nanobelts and nanorods has been successfully synthesized by using wet oxidation technique [65][66]. The setup and parameters such as temperature and pressure may vary, but the method does exhibit a common element. This common element is the employment of water vapor. Thus, the name wet oxidation. The advantages of wet oxidation are low cost, simple to fabricate, environment friendly and catalyst-free [18][56]. Moreover, the nanostructure produced by this technique can have a strong adhesion to the substrate and high plasticity [56][65]. The creation of nanostructure was believed to be dependent on the temperature during oxidation, and wet oxidation time [56]. Wet oxidation is preferred instead of dry oxidation because wet oxidation ensures a non-planar growth of ZnO [56], while dry oxidation only encourages planar and dense ZnO grains. It has been shown by Z.W.Li and coworkers that the growth of ZnO nanostructures is in fact affected by water vapor [66]. Furthermore, according to C.H Xu et al., the amount of water vapor in the environment will affect the PL luminescence and resistivity of the oxide formed [67].

### 2.3.2 Hydrothermal

Hydrothermal is another preferred method used to grow ZnO nanostructures by many scientists [68–70]. Hydrothermal method comes with the benefits of inexpensive, simpler, ecofriendly, and low temperature requirement. However, this method required a closed system and the presence of relatively high vapor pressure (higher than atmospheric pressure) [71–73]. In this hydrothermal synthesis method, water is used as solvent because it is a polar solvent [74], which means water can be attracted to either negative or positive charged of an atom. The polarity of water comes from the bent shape of water molecules. Furthermore, the polarity of water could be modified by changing the temperature and pressure [74]. Thus, water as solvent has an advantage over any other type of solvents. Typically, hydrothermal method involves two main steps which is seeding of seed layer and growing of nanostructure. Although seeding is not necessary for the growing of ZnO nanostructure, it is still done by many researchers as it will affect the nanostructure's shape and alignment [75]. The seeding steps could be done by sputtering [68], chemical spray pyrolysis (CSP) technique [72] or seeding solution [76]. The seeding solution used often is a mixture of zinc acetate and other solutions [76–80]. While the growth step of hydrothermal involved dipping of substrate in growth solution. Classically, the growth solution used is prepared by mixing zinc nitrate and hexamethylenetetramine (HMTA) [78][79]. The substrate is then rinsed with distilled water and then undergoes annealing process. According to the work of N.F Idris and coworkers [76], the best growth duration under hydrothermal method for highest density of nanorods is 10 hours. In the same work, it also reveals that the growth duration will affect the length of ZnO nanorods.

### 2.3.3 Chemical Bath Deposition

Unlike other gas-based synthesis method [81-85], chemical bath deposition is a solution-based synthesis method same as hydrothermal method. Thus, they both exhibit some similarities. Compared to the hydrothermal method, CBD could be carried out in open area under atmospheric pressure which means that CBD doesn't require high pressure environment for the operation. CBD method has been demonstrated in many works on different substrates including Teflon, glass, PET, and porous p-type Si to find out the characterization of ZnO nanostructure [17][86][38][39][57]. CBD technique has the advantages of good uniformity, capability of large scales fabrication, low cost, and simple setup [17][86]. This method can also control the chemical composition and ensure the homogeneity of solution [17]. Typically, the CBD technique employed in three steps. Firstly, the substrate is cleaned in ultrasonic bath with acetone/isopropyl alcohol/ethanol. Secondly, ZnO seed layer is grown on the substrate with sputtering. Growing of seed layer is to provide a nucleation site for the growing of nanostructures so it can optimize the nucleation rate or a specific growth direction. However, as stated before, a seed layer is not necessary in growing ZnO nanostructure. The present of seeding has an impact on the density of ZnO nanostructure grown [87]. Nonetheless, seeding is needed for oriented growth of nanostructure as stated by author of [88]. The seed layer is then passed through annealing process, this process improves the crystallinity of the ZnO seed layer and the adhesion on the substrate [89], which contributes to well-aligned ZnO nanostructures. The third step is to grow nanostructures on the seed layer/substrate. The substrate is immersed in an aqueous solution that contains salt of metal, in this case Zn and a complexing agent/ligand (eg: ammonia, HMTA). The substrate is placed vertically in the beaker



containing the solution. The beaker is then placed in oven at a higher temperature for continuous heating for the desired growth time. After that the sample is then rinsed with distilled water. ZnO nanostructures grown by CBD are affected by several parameters such as thickness of seed layer, concentration of precursor solution, pH of the solution, growth temperature and growth time. For example, the diameter and length of ZnO nanostructure can be adjusted by modulating the precursor concentration and growth temperature [39][90]. Besides, increasing the pH value of precursor will destroy the hexagonal wurtzite shape of ZnO nanorod formed [91]. Due to the simplicity and advantages provided by this method, CBD is chosen as a growing technique in this work. Hence, further discussion of CBD will be presented in the next section.

## 2.4 Growth Mechanism

There are three steps involved in growing nanostructure by CBD. These three steps are as following:

- i) Formation of ionic substance, in this case  $Zn^{2+}$  as in equation 2.4
- ii) Transportation of ionic substance formed in a solution
- iii) Condensation of these substance as in equation 2.7

